Biosensors and Bioelectronics 97 (2017) 59–64

Contents lists available at ScienceDirect

Biosensors and Bioelectronics

journal homepage: www.elsevier.com/locate/bios

Ultrasensitive detection of aflatoxin B_1 by SERS aptasensor based on exonuclease-assisted recycling amplification

Qin Li[1], Zhicheng Lu[1], Xuecai Tan, Xiaoyan Xiao, Pan Wang, Long Wu, Kang Shao, Wenmin Yin, Heyou Han[*]

State Key Laboratory of Agricultural Microbiology, College of Science, Huazhong Agricultural University, Wuhan 430070, PR China

ARTICLE INFO

Keywords:
Aflatoxin B_1
Aptamer
Exonuclease III
Recycling amplification
Surface enhanced Raman scattering

ABSTRACT

Aflatoxin B_1 (AFB_1) is one of the most abundant and carcinogenic food-contaminating mycotoxins around the world. In this study, we proposed a surface enhanced Raman scattering (SERS) sensing strategy for the determination of AFB_1. An aptamer for AFB_1 partially hybridized with complementary-DNA, which was released after the recognition of AFB_1 and immediately hybridized with hairpin DNA on the surface of sputtering Au film. Exonuclease III hydrolyzed the double-stranded DNA, leaving short single-stranded DNA on the Au surface and releasing complementary-DNA for next ring opening and digestion. SERS tag was captured on Au surface by DNA hybridization. Agarose gel electrophoresis and dynamic light scattering showed that SERS tag was successfully prepared. The detection principle was validated by electrochemical impedance spectroscopy and SERS at each step. High sensitivity and good selectivity for AFB_1 detection were observed. The results showed that there was a good linear relation when the AFB_1 concentration was from 1×10^{-6} to 1 ng/mL, and the limit of detection (LOD) was 0.4 fg/mL. This sensor was also applied for quantifying AFB_1 levels in spiked peanuts samples, the recoveries was in the range of 89–121%.

1. Introduction

Mycotoxins are a group of secondary fungal metabolites produced by different species of filamentous fungi (Wang et al., 2014) and cause serious threats to food security (Bedard and Massey, 2006) because they can damage the immune system, nervous system and reproductive system of humans and animals (Koppen et al., 2010). Among various types of mycotoxins, aflatoxin B_1 (AFB_1) has the strongest effects of carcinogenesis and mutagenesis (Groopman et al., 1981). Therefore, developing a rapid, simple and sensitive method for AFB_1 detection is highly necessary and urgent for food safety.

Chromatography methods, such as thin layer chromatography (Klaric et al., 2009), high-performance liquid chromatography (HPLC) (Algul and Kara, 2014; Nguyen et al., 2007) and liquid chromatography combined with mass spectrometry (LC-MS) (Warth et al., 2014), have been developed for the detection of AFB_1 with LOD in the range of dozens to several hundred nanograms per gram. Immunoassays based on specific recognization between antibodies and AFB_1, such as enzyme-linked immunosorbent assay (ELISA) (Liu et al., 2013a), fluorescence immunoassay (Wang et al., 2016), immunochromatography assay (Urusov et al., 2014), and immunosensors (Daly et al., 2000; Basu et al., 2015; Ma et al., 2016), have been considered as promising strategies because they provide the possibility of on-site test. However, the low detection sensitivity and difficulty in the preparation of antibodies for small molecules have largely hindered the wide application of immunoassays of AFB_1 when both sensitivity and stability are required. Therefore, it is highly necessary to develop reliable sensors with high sensitivity for on-site detection of AFB_1.

Compared with conventional detection methods, surface enhanced Raman scattering (SERS) is a nondestructive and noninvasive technique which requires the minimal sample preparation (Wang et al., 2013). SERS is a molecular spectroscopy method that provides abundant structural information. Meanwhile, the substantial enhancement of Raman signals makes SERS a well-established ultrasensitive analytical tool (Alvarez-Puebla and Liz-Marzan, 2010). Based on these unique features, label-free SERS method has been successfully applied in the detection of biotoxins, including saxitoxin (Huai et al., 2013), domoic acid (Olson et al., 2011) and aflatoxin (Wu et al., 2012; Lee et al., 2014). In direct SERS detection, it is critical to extract useful information from complicated Raman spectra that originate from the co-adsorption of matrix and the non-selectivity of SERS. Therefore, chemometric models based on statistical methods are often used to

* Corresponding author.
E-mail address: hyhan@mail.hzau.edu.cn (H. Han).
[1] Equal contribution.

http://dx.doi.org/10.1016/j.bios.2017.05.031
Received 27 February 2017; Received in revised form 9 May 2017; Accepted 17 May 2017
Available online 17 May 2017
0956-5663/ © 2017 Elsevier B.V. All rights reserved.

process the data in direct SERS detection (Lee et al., 2014). In terms of selectivity, labeled SERS detection strategies have advantages of both high sensitivity and specific selectivity (Ganbold et al., 2014; Li et al., 2016; Zhao et al., 2015); besides, the use of SERS tags, which provide unambiguous Raman signals of tag molecules, largely reduces the difficulty in data processing. For example, immunoassay detections of zearalenone (Liu et al., 2014) and aflatoxin B_1(Fang et al., 2016; Ko et al., 2015) have been proved to be highly flexible and sensitive. However, the preparation of specific antibodies for small molecule toxins provides great possibilities to improve the analytical performance (He et al., 2014). In comparison to natural antibodies, aptamers, which are also called artificial antibodies, have been very promising candidates in the construction of biosensors and chemical sensors due to their stability, specificity and ease of use (Song et al., 2008).

Exonuclease III (Exo III), a sequence-independent nuclease, could specifically hydrolyze mononucleotide from its blunt ends (5'-overhangs or nicks of duplex DNA), and gradually remove mononucleotide from the 3'-end (Liu et al., 2013b; Wang et al., 2015). This feature of selective nucleotide digestion of Exo III may be utilized as an effective catalytic tool for the amplified detection of DNA, leading to significant enhancement of detectable signals and higher sensitivity.

In the present study, we proposed a highly sensitive sensing strategy for SERS determination of AFB_1 by integrating the amplification of Exo III-catalyzed target recycling with the specific recognition of aptamer DNA. As illustrated in Scheme 1, four types of DNA were involved in our experiment design. The first type was the aptamer DNA of AFB_1. The second type of DNA, which could be released at the presence of AFB_1, was partially complementary to aptamer DNA. The third type was a hairpin DNA which was hydrolyzed by Exo III at a restriction site after hybridizing with the second type DNA, leaving short single-stranded DNA on surface to capture Raman tags via hybridization with the fourth DNA, a sequence of oligonucleotides on the surface of Raman tags. The released second type of DNA participated in the subsequent cycles, leading to the fact that a large number of Raman probes could be anchored on the surface of gold-coated glass slides by forming double-stranded DNA in the enzyme-cycling amplification process. Each step of the detection was validated, and the proposed exonuclease-assisted sensing method was demonstrated to be a rapid, simple and inexpensive tool for AFB_1 determination.

2. Materials and methods

2.1. Materials

$HAuCl_4 \cdot 4H_2O$, trisodium citrate dihydrate, ethylenediaminetetraacetic acid (EDTA), tris-(2-carboxyethyl) phosphine hydrochloride (TCEP-HCl) were purchased from Sinopharm Chemical Reagent Co., Ltd. (Shanghai, China). Aflatoxin B_1 (AFB_1), aflatoxin B_2 (AFB_2), aflatoxin G_1 (AFG_1), aflatoxin G_2 (AFG_2), aflatoxin M_1 (AFM_1), deoxynivalenol (DON), zearalenone (ZON), tris (2-carboxyethyl) phosphin hydrochloride (TCEP), 4-Nitrothiophenol (4-NTP) and agarose (for routine use) were obtained from Sigma-Aldrich. Exonuclease III and the master buffer (10× NEBuffer1, 100 mM Bis Tirs propane-HCl,100 mM $MgCl_2$, 10 mM DTT, pH 7.0) were purchased from New England Biolabs (Beijing) LTD. All the reagents were used as received without further purification. 6-mercapto-1-hexanol (MCH) was from J & K Chemical Ltd. (Beijing, China). Milli-Q water was used throughout the experimentation.

1× TE buffer for DNA dissolution was prepared by mixing 10 mM Tris-HCl, 1 mM EDTA (pH = 7.4) and 10 mM TCEP. 5× TBE stock solution contained 450 mM Tris-boric acid and 10 mM EDTA (pH = 8.0). Aging buffer 1 was 0.1 M PBS containing 0.1% SDS and aging buffer 2 was 0.01 M PBS containing 2 M NaCl and 0.01% SDS (pH = 7.4).

All of the DNA sequences with HPLC purification were purchased from Sangon Biological Engineering Technology & Co., Ltd (Shanghai, China). The sequences are as follows:

Aptamer DNA: 5'-GTT GGG CAC GTG TTG TCT CTC TGT GTC TCG TGC CCT TCG CTA GGC CC-3'.

Hairpin DNA: 5'-HS-$(CH_2)_6$-TTT TTG TGC CCA ACA TTC CAC CTA TTG CCT GTT GGG CAC GTG T-3'.

Complementary DNA: 5'-ACA CGT GCC CAA CAG GCA AT A GGC TCA C-3'.

Capture DNA: 5'-HS-$(CH_2)_6$-TTT TTT GTT GGG-3'.

2.2. Instrumentation

Raman spectra were obtained on a inVia Raman spectrometer (Renishaw, UK) with a 633 nm He-Ne laser working at 10 mW. Raman spectra were recorded with 10 s accumulation time and a 20×

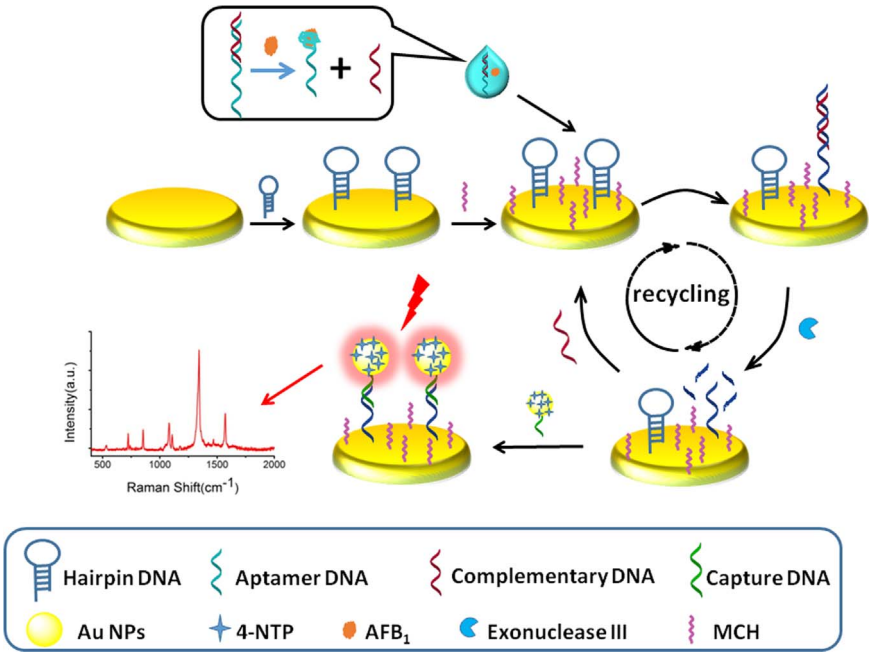

Scheme 1. Schematic illustration of the SERS aptasensor for aflatoxin B_1 detection.

objective. The average of spectra from 5 randomly selected spots was used in Raman experiment.

UV–vis absorption spectra of aqueous solution were obtained on a Nicolet Evolution 300 UV–vis spectrometer (Thermo Nicolet, America) using 1 cm optical path cell. UV–vis spectra on solid surface were recorded with an optical fiber spectrometer (QE 65Pro, Ocean Optics, Inc.) in the reflection mode. Transmission electron microscopy (TEM) images were acquired by a JEM-2010 transmission electron microscope (JEOL, Japan). Surface morphology was characterized with a Hitachi SU8010 field-emission scanning electron microscope (FE-SEM). A Zetasizer Nano ZS90 DLS system (Malvern, England) was used to measure hydrodynamic diameters. An OCA15EC optical contact angle measuring system was use to characterize the contact angle of water on Au film. The gel was run in a horizontal electrophoresis system (DYCP-31DN Electrophoresis Cell, BEIJING LIUYI BIOTECHNOLOGY CO., LTD.; electrode space, 20 cm). Electrochemical impedance spectroscopy (EIS) was performed by an electrochemical workstation (CHI660D instruments, Shanghai Chenhua Instrument Corp., Shanghai, China).

2.3. Preparation of Au nanoparticles SERS probe

The Raman probe was obtained by capping the capture DNA and 4-Nitrothiophenol (4-NTP) on the surface of Au nanoparticles (Au NPs). Au NPs were synthesized according to the method of Frens (1973). Briefly, 50 mL of 0.01% $HAuCl_4$ aqueous solution was heated to boiling with vigorous stirring. Then, 1 mL of freshly prepared 1% trisodium citrate solution was added rapidly, resulting in a color change from light yellow to faintly blue and to wine red ultimately. The boiling was continued for another 30 min to complete the reduction. The solution was cooled down to room temperature and stored at 4 °C. For modification of Au NPs with capture DNA, 5 μL of 100 μM capture DNA in 1× TE was added to 1 mL Au NPs solution under vigorous stirring for 5 min. The solution was incubated at 25 °C for 12 h (Chen et al., 2014). Next, aging buffer 1 was added into the solution to a final PBS and SDS concentration of 10 mM and 0.01%, respectively. After that, 1 mM 4-NTP ethanol solution was added at a final concentration of 10 μM for another 3 h. Subsequently, the 4-NTP/DNA/Au NPs conjugates were aged in a salt solution containing 0.05 M NaCl, 10 mM PBS and 0.01% SDS for 6 h. Finally, Au NPs solution was centrifuged at 8000 rpm for 8 min and resuspended in phosphate buffer (10 mM; pH=7.4) for three times to remove the unbound capture DNA and 4-NTP. The modified Au NPs solution was stored at 4 °C for further use. For stability investigation, 2 M NaCl and 2 M HCl were respectively used to adjust the ionic strength and pH of the dispersion of Au nanoparticle SERS probe.

For nanoparticle gel electrophoresis, agarose gels were prepared with and immersed in 0.5× TBE buffer (prepared by diluting 5× TBE stock solution). The electrophoresis voltage was set to 120 V and the time was 30 min. Gel images were recorded with a digital camera and only a small linear contrast adjustment was applied to the images in order to give a true visual representation of the gel appearance.

2.4. Self-assembly of hairpin DNA on gold-coated glass slides

The detailed procedures for the preparation of gold-coated glass slides were listed in the first section of Supplementary information. After fabrication, gold-coated glass slides were covered with a PET film on which 24 regularly arranged circular holes (diameter=3 mm) were punched. The hairpin DNA was heated to 95 °C for 5 min, then cooled at a rate of 0.1 °C/s to 25 °C to construct the stem-loop structure after 1 h activation by 10 mM TCEP which cut the S-S bond. The annealed hairpin DNA (5 μL, 1 μM) was dripped into the holes to assemble on the gold films by formation Au-S bond for 12 h in a humidity box at room temperature. Unbound hairpin DNA was washed away with ultrapure water. The exposed gold film at the hole was then blocked with 1 mM MCH for 1 h, washed thoroughly with ultrapure water and dried under nitrogen stream.

2.5. AFB_1 detection

AFB_1 aptamer DNA and complementary DNA sequence formed double-stranded DNA (ds-DNA) after the annealing treatment. To investigate the time effect on AFB_1 competition and hairpin opening, 5 μL of 1 μM ds-DNA and 5 μL of 1 ng/mL AFB_1 solution were dropped into different holes for different incubation time. After being washed with 10 mM PBS, the holes were covered by 5 μL 1× NE buffer1 containing 1 U Exo III at 37 °C for 1 h, followed by washing with 0.01 M PBS and drying with N_2. Next, 5 μL of Raman probes were added into each hole with 1 h incubation time followed by rinsing with 0.01 M PBS and drying under N_2 stream. In the optimization of exonuclease-assisted recycling amplification, only the incubation time of exonuclease was systematically changed with other condition as the same as that in the first optimization testing. In surveying immobilization of SERS probe, the incubation time of Rama probe was variable with other conditions being constant. AFB_1 detection was performed under the optimum conditions.

2.6. Specificity analysis

Mycotoxins AFB_2, AFM_1, AFG_1, AFG_2, DON and ZON were selected to test the specificity of this assay method. All mycotoxins were detected at 10 ng/mL concentration. Other detection conditions were identical to those used in the AFB_1 procedure.

2.7. Real sample detection

The peanut samples were fully ground by hand after drying and weighed into 1 g per sample. 2 mL of methanol/water (volume ratio, 80: 20) was added followed by sonication for 30 min to assist the extraction performance. Then, these samples were further centrifuged for 20 min at 12,000 r/min. Finally, 1 mL supernatant was collected and transferred into other centrifugal tubes. Then, AFB_1 standard samples at three concentrations (0.01, 0.1 and 1 pg/mL) were added, which were used as real samples for detection with the above constructed method.

3. Results and discussion

3.1. Preparation and characterization of Au NPs SERS probe

As shown in Fig. 1A, after modification of capture DNA and 4-NTP, the absorption spectrum of SERS probes showed a maximum extinction peak at 521 nm, which was 2 nm red shift to the original Au NPs the extinction spectrum of which centered at 519 nm. It is known that the absorption spectra of novel metal nanoparticles are highly sensitive to dielectric constant. Therefore, the shift in the absorption spectra of Raman probes indicates that capture DNA and 4-NTP were adsorbed on gold nanoparticle surface and altered the dielectric constant around the Au nanoparticle. Fig. 1B reveals that the hydrodynamic diameters of Au NPs increased from 15 nm to 18 nm after conjugation with capture DNA. TEM image in Fig. S1A shows that Au NPs have an average diameter of 15 nm. The zeta potentials of Au nanoparticles and SERS probe are shown in Fig. S1B. The surface of Au NPs was always at the negative potential regardless of the surface modification.

The surface modification of Au NPs was optimized to obtain stable SERS probes with high performance simultaneously. The concentration of Au NPs was calculated to be about 2 nM according to the method reported by Haiss et al. (2007). The effect of molar ratio between capture DNA and Au NPs was investigated using uv–vis spectroscopy and showed in Fig. S2. The absorption spectra of Au SERS probe become unchanged when the ration of capture DNA to Au NPs was

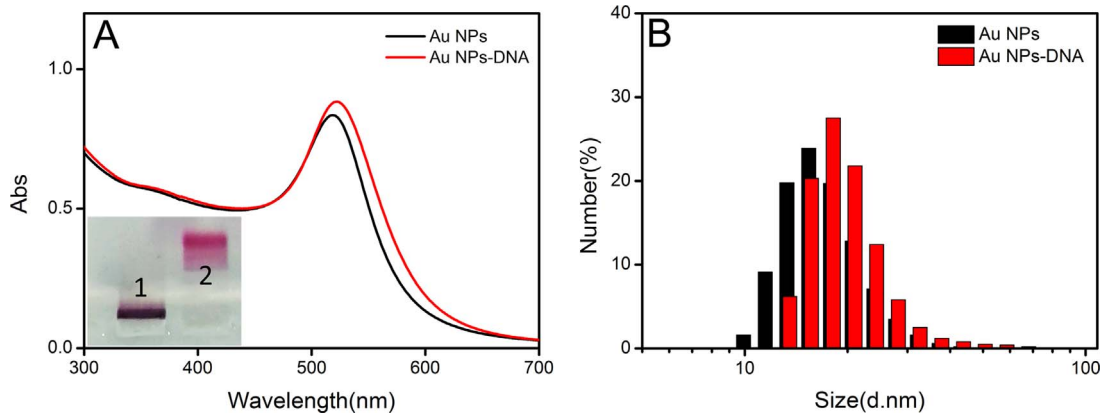

Fig. 1. (A) UV–Vis spectra of Au NPs and Au NPs-DNA. The inserted image is the electrophoresis result of DNA modification on Au NPs. Lane 1: pure Au NPs; Lane 2: signal-DNA modified Au NPs. (B) Hydrodynamic size of Au NPs and Au NPs-DNA.

higher than 200. A slightly larger value was determined in modification of Au NPs to ensure a sufficient stability of the SERS probe. Fig. S2B shows a SERS demonstration of 4-NTP modification on Au NPs. As shown, bare and capture DNA modified Au NPs gave a baseline level Raman signal. In contrast, 4-NTP modified Au NPs produced a strong Raman signal belonging to it. The influence of 4-NTP concentration on signal intensity of the SERS probe was showed in Fig. S2C. As can be seen, Raman signal became saturated when the ration of 4-NTP:Au NPS was larger than 5000. Therefore, the optimum ratio of Au NPs: capture DNA: 4-NTP in preparation of Au based SERS probe was determined to be 1: 250: 5000. The Au NPs-based SERS probe was stable in wide range ionic strength and pH as showed in Fig. S3, Table S1 and Fig. S4.

Additionally, modification of Au NPs with capture DNA was investigated by agarose gel electrophoresis and the digital image was presented in the inset of Fig. 1A. Bare Au NPs corresponded to lane 1 (lane 1). As shown, Au NPs aggregated into violet sediments under the condition of high salt concentration and could not migrate into the gel due to the electrostatic screening effect (Pellegrino et al., 2007). In contrast, after modification with capture DNA and Raman probes, the Au NPs/capture DNA/4-NTP conjugate showed good stability and migrated into the gel even under the same high ionic strength (lane 2), indicating successful assembly of capture DNA and Raman probes on the Au NPs surface.

3.2. Surface functionalization of gold chip

Fig. 2 shows the digital photo of the SERS chip. The chip was made by depositing gold film (1 μm in thickness as shown in Fig. S5A) on glass slide and pasting a PET film (0.18 mm thick shown in Fig. S5B) with 24 regularly arranged circular holes. Part of the Au film was exposed in the round hole area and isolated from each other by the continuous PET film. The round Au areas were used as the experimental zones. The surrounding PET film was more hydrophobic than Au film because the water contact angle of PET was 15° larger than that of Au film as shown Fig. S6 and was used for controlling the spreading area of solution, ensuring consistent reaction conditions at each hole region.

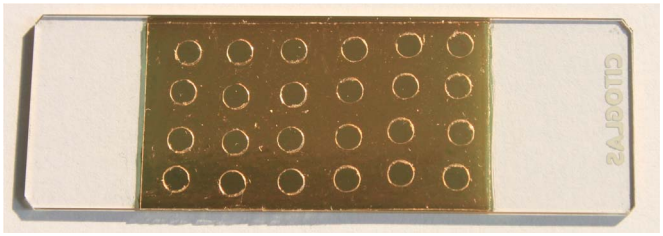

Fig. 2. Digital photo of the chip. The circular areas were used for hairpin DNA modification.

3.3. Feasibility test of assay protocol

To validate the detection protocol, electrochemical impedance spectroscopy (EIS) was performed at each modification and recognition step of the aptasensor on gold disk electrode with all other conditions being the same as on Au film and the result was given in Fig. 3A. Curve a showed a very low electron transfer resistance of the electroactive probe $[Fe(CN)_6]^{3-/4-}$. As expected, immobilization of hairpin-DNA and blocking with MCH on gold electrode surface increased R_{et} (the semicircle portion), because the negative charge layer of phosphate skeleton of hairpin DNA hindered the diffusion of electroactive $[Fe(CN)_6]^{3-/4-}$, a probe with the same charge. The increase of R_{et} indicates that hairpin DNA and the blocking reagent could perform their functions well, which ensures the feasibility and reliability of the aptasensor. After the addition of AFB_1, double-stranded DNA (formed by AFB_1 aptamer and partially complementary sequence), and exonuclease, the ring opening of hairpin and cutting of double-stranded DNA reduced the surface electron transfer resistance, as shown by curve d in Fig. 3A. The further decrease of R_{et} after capturing of Raman tags could be attributed to the enhancement effect of Au nanoparticles on electron conduction. The uv–vis spectra obtained on aptasensors having been used to detect AFB_1 from 10^{-6} to 1 ng/mL was given in Fig. S7A and revealed a gradual increment in absorbance, indicating the increment in amount of captured Au SERS probe. An SEM image of the aptasensor used for detection of 1 ng/mL AFB_1 was given in Fig. S7B and showed a large amount of Au on a rough surface, providing an intuitive proof of the realization of the sensing principle.

The feasibility of the proposed method was also evaluated by recording 4-NTP SERS signals in a series of control experiments, where a certain component of the aptasensor was intentionally made absent each time, including hairpin DNA, aptamer DNA-complementary DNA, AFB_1, EXO III and Raman probe. As shown in Fig. 3B, no Raman signal could be detected when Raman probe was absent. In the absence of any other components, SERS signal could be detected, but the intensity was significantly lower than that recorded on the sensor constructed with all components. Ideally, SERS signal could be detected only in the presence of AFB_1. However, curves b-e reveal that there is nonspecific adsorption with different signal intensities depending on the construction components. In the absence of hairpin DNA, Raman probe had the smallest adsorption amount on MCH-blocked Au film, resulting in a weakest SERS signal. In the presence of hairpin DNA, the SERS signals were nearly the same as long as the loop of hairpin DNA remained closed (curve c and d). By contrast, opening of the hairpin DNA loop, as shown by curve b, resulted in more intense nonspecific SERS signals, which may be due to that ring opening exposed the complimentary sequence of

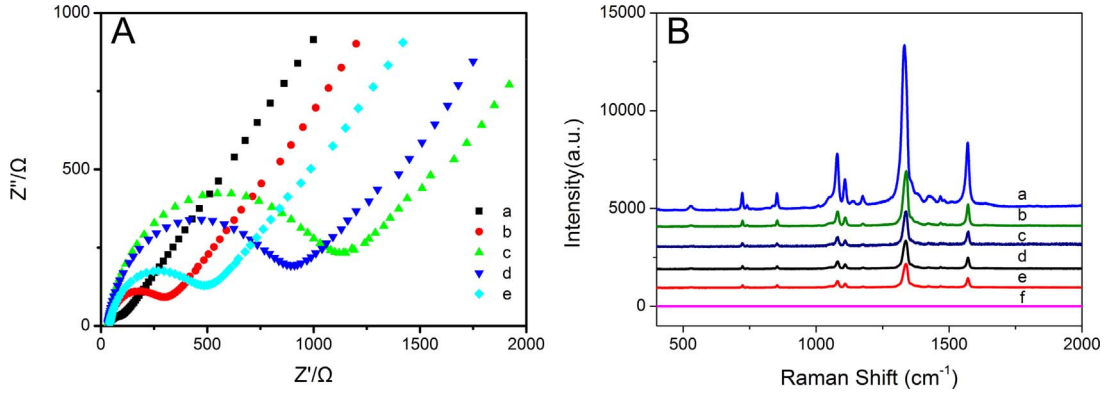

Fig. 3. Feasibility test of the AFB_1 sensor. (A) EIS results recorded on electrode surface in different functionalization steps: a) bare, b) hairpin, c) blocking, d) recycling amplification, e) Au NPs. (B) SERS spectra obtained in a series of control experiments: a) hairpin DNA, EXO III, aptamer-complementary DNA, AFB_1 and SERS tag; b) hairpin DNA, aptamer-complementary DNA, AFB_1 and SERS tag; c) hairpin DNA, EXO III, AFB_1 and SERS tag; d) hairpin DNA, EXO III, aptamer-complementary DNA and SERS tag; e) EXO III, aptamer-complementary DNA, AFB_1 and SERS tag; f) hairpin DNA, EXO III, aptamer-complementary DNA and AFB_1. The concentration of AFB_1 was 1 ng/mL.

capture DNA and a part of Raman probes were specifically captured besides the nonspecifically adsorbed probes. The long-term stability of the sensor was assessed by surveying the detection performance of the chip for 1 ng/mL AFB_1 with time span up to 20 days. A batch of gold chips prepared at the same condition keep in sealed tubes which were filled with nitrogen were stored at 4 °C. The result was given in Fig. S8 and showed that the SERS chips maintained nearly the same detective ability. The reason was that the hairpin DNA was stable at a low temperature (4 °C) and SERS signals come from Au NPs SERS probe, having no relation with the gold film.

3.4. Specificity analysis

Six types of mycotoxins, including DON, ZON, AFM_1, AFB_2, AFG_1, and AFG_2, were selected as negative controls to test the specificity of this method. As indicated in Fig. 4, the intensities of SERS signals of all the six types of mycotoxins were at the level of blank sample at the concentration of 10 ng/mL. In contrast, SERS intensity for AFB_1 detection was more than three folds higher than that for negative controls, even though the concentration of AFB_1 was four orders of magnitude lower than that of the negative controls. The results indicate that the aptasensor has perfect specificity to AFB_1 based on the specific recognition of aptamer for AFB_1. The highly repeatable results obtained here along with constant nonspecific signals demonstrate the feasibility of the proposed method for quantitative detection of AFB_1.

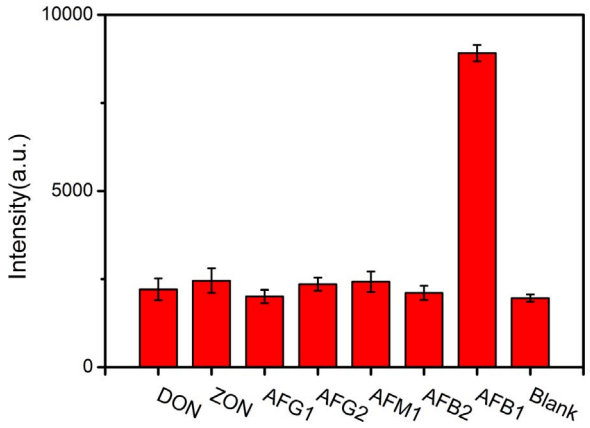

Fig. 4. Confirmation of the specificity of the aptasensor to AFB_1, AFB_2, AFM_1, AFG_1, AFG_2, DON and ZON. The concentration of AFB_1 was 10^{-3} ng/mL and that of other samples was 10 ng/mL. Error bars show the standard deviation of three experiments.

3.5. SERS detection of AFB_1

The whole detection time using the aptasensor, concerning the competitive recognition AFB_1 and release of complimentary DNA, exonuclease-assisted recycling amplification, and capture of Raman probe, was optimized. The survey result of the first step was shown in Fig. S9A and displayed that at least one hour reaction time was required to get a Raman signal strong enough. In Fig. S9B, the optimum of recycling amplification duration, the integral area of Raman peak rapidly increased until 1 h, after which Raman signal changed slowly even though the recycling amplification time was doubled. The inspection of immobilization of Raman probe to the chip surface was shown in Fig. S9C. The signal got the maximum value after a forty minutes of incubation time. Therefore, the whole detection time, in order to get the best detection performance, was about 3 h along with the times consumed by cleaning steps between each operation. The relative long detection time may hinder the application of the aptasensor in on-site detection to a certain degree. However, a compromise solution between the detection performance and the whole detection time may also be desirable for the rapid testing application.

Fig. 5A shows the signal-amplified SERS detection of AFB_1. The Raman intensity increased with increasing concentration of AFB_1, because higher AFB_1 concentration increased the release of complementary-ssDNA, which acted as the primer in the digestion amplification process and enhanced the capture of Raman probes. Fig. 5B shows that the integral area of Raman peak at 1334 cm^{-1} was linear with the AFB_1 concentrations ranging from 1×10^{-6} to 1 ng/mL. The linear regression equation was y=333875+43746 lg x with the correlation coefficient R^2=0.9889, where y is the integral area of Rama peak at 1334 cm^{-1} and x is AFB_1 concentration. The limit of detection (LOD) (Zhao et al., 2015) of AFB_1 (S/N=3) was 0.4 fg/mL. Compared with the results reported in literatures, this work indicated an excellent sensitivity for AFB_1 detection (Table S2). The recovery experiments of AFB_1 in peanut samples were performed to confirm the practical application of the aptasensor and the results are presented in Table S3. The recovery rate was measured by spiking 1,10,100 pg/mL of the target AFB_1 into the peanut samples and calculating the found amount/added amount ratio. As shown in Table S2, the recovery rate was 89–121%. The recovery had a large deviation at high spiking concentration. From SEM results, the reason arose from the fact that more Raman probes resulted in the approaching of Au nanoparticles to each other and Raman signal molecules in the close-proximity region provide more intensity than the Raman signal molecules on well distributed Au nanoparticles.

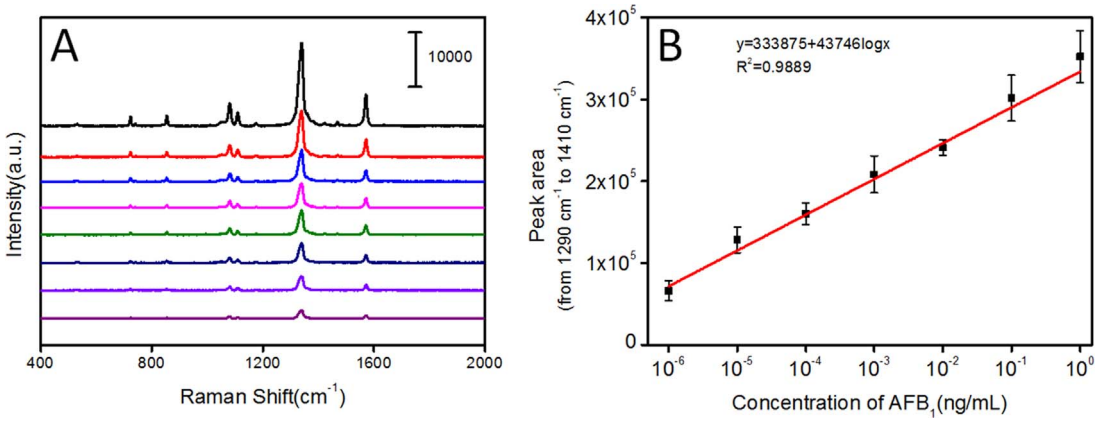

Fig. 5. SERS spectra (A) and calibration curve (B) of the aptasensor for AFB_1 at different concentrations. The concentration of AFB_1 is 1, 10^{-1}, 10^{-2}, 10^{-3}, 10^{-4}, 10^{-5}, 10^{-6} and 0 ng/mL from top to bottom in (A). Error bars in (B) show the standard deviation of three experiments.

4. Conclusions

An aptamer-SERS sensing chip was successfully constructed for the detection of AFB_1. The specific recognition of aptamer for AFB_1 as well as the exonuclease-assisted recycling amplification and SERS signal enhancement ensure the specificity and sensitivity of the method. The linear range was determined to be 1×10^{-6} to 1 ng/mL and the LOD was calculated to be 0.4 fg/mL. The aptasensor developed here is highly promising for portable use because some complex operations can be pre-completed, such as chip functionalization, SERS tag preparation, and aptamer-complementary DNA hybridization, and only some simple operations, such as sample adding and washing, are needed to be carried out in the detection. This study provides important implications for the development of more rapid and portable aptasensors for the determination of mycotoxins.

Acknowledgements

We gratefully acknowledge the financial support from National Key R & D Program (2016YFD0500706) and National Natural Science Foundation of China (21375043).

Appendix A. Supplementary material

Supplementary data associated with this article can be found in the online version at http://dx.doi.org/10.1016/j.bios.2017.05.031.

References

Algul, I., Kara, D., 2014. Food Chem. 157, 70–76.
Alvarez-Puebla, R.A., Liz-Marzan, L.M., 2010. Small 6, 604–610.
Basu, J., Datta, S., RoyChaudhuri, C., 2015. Biosens. Bioelectron. 68, 544–549.
Bedard, L.L., Massey, T.E., 2006. Cancer Lett. 241, 174–183.
Chen, K., Wu, L., Jiang, X., Lu, Z., Han, H., 2014. Biosens. Bioelectron. 62, 196–200.
Daly, S.J., Keating, G.J., Dillon, P.P., Manning, B.M., O'Kennedy, R., Lee, H.A., Morgan, M.R., 2000. Food Chem. 48, 5097–5104.
Fang, C., Wei, C., Xu, M., Yuan, Y., Gu, R., Yao, J., 2016. RSC Adv. 6, 61325–61333.
Frens, G., 1973. Nature 241, 20–22.
Ganbold, E.-O., Lee, C.M., Cho, E.-M., Son, S.J., Kim, S., Joo, S.-W., Yang, S.I., 2014. Anal. Methods 6, 3573–3577.
Groopman, J.D., Croy, R.G., Wogan, G.N., 1981. Proc. Natl. Acad. Sci. USA 78, 5445–5449.
Haiss, W., Thanh, N.T.K., Aveyard, J., Fernig, D.G., 2007. Anal. Chem. 79, 4215–4221.
He, T., Wang, Y., Li, P., Zhang, Q., Lei, J., Zhang, Z., Ding, X., Zhou, H., Zhang, W., 2014. Anal. Chem. 86, 8873–8880.
Huai, Q., Gao, C., Miao, J., Yao, H., Wang, Z., 2013. Anal. Methods 5, 6870–6873.
Klaric, M.S., Cvetnic, Z., Pepeljnjak, S., Kosalec, I., 2009. Arh. Hig. Rada Toksikol. 60, 427–434.
Ko, J., Lee, C., Choo, J., 2015. J. Hazard. Mater. 285, 11–17.
Koppen, R., Koch, M., Siegel, D., Merkel, S., Maul, R., Nehls, I., 2010. Appl. Microbiol. Biotechnol. 86, 1595–1612.
Lee, K.-M., Herrman, T.J., Bisrat, Y., Murray, S.C., 2014. J. Agric. Food Chem. 62, 4466–4474.
Li, A., Tang, L., Song, D., Song, S., Ma, W., Xu, L., Kuang, H., Wu, X., Liu, L., Chen, X., Xu, C., 2016. Nanoscale 8, 1873–1878.
Liu, B.H., Hsu, Y.T., Lu, C.C., Yu, F.Y., 2013a. Food Control 30, 184–189.
Liu, J., Hu, Y., Zhu, G., Zhou, X., Jia, L., Zhang, T., 2014. J. Agric. Food Chem. 62, 8325–8332.
Liu, S., Wang, Y., Zhang, C., Lin, Y., Li, F., 2013b. Chem. Commun. 49, 2335–2337.
Ma, H., Sun, J., Zhang, Y., Bian, C., Xia, S., Zhen, T., 2016. Biosens. Bioelectron. 80, 222–229.
Nguyen, M.T., Tozlovanu, M., Tran, T.L., Pfohl-Leszkowicz, A., 2007. Food Chem. 105, 42–47.
Olson, T.Y., Schwartzberg, A.M., Liu, J.L., Zhang, J.Z., 2011. Appl. Spectrosc. 65, 159–164.
Pellegrino, T., Sperling, R.A., Alivisatos, A.P., Parak, W.J., 2007. J. Biomed. Biotechnol. 2007, 26796.
Song, S., Wang, L., Li, J., Fan, C., Zhao, J., 2008. TrAC Trends Anal. Chem. 27, 108–117.
Urusov, A.E., Zherdev, A.V., Dzantiev, B.B., 2014. Microchim. Acta 181, 1939–1946.
Wang, D., Zhang, Z., Li, P., Zhang, Q., Zhang, W., 2016. Sensors 16, 1094.
Wang, Y., Bai, X., Wen, W., Zhang, X., Wang, S., 2015. ACS Appl. Mater. Interfaces 7, 18872–18879.
Wang, Y., Yan, B., Chen, L., 2013. Chem. Rev. 113, 1391–1428.
Wang, Y., Zhang, Y., Su, Y., Li, F., Ma, H., Li, H., Du, B., Wei, Q., 2014. Talanta 124, 60–66.
Warth, B., Petchkongkaew, A., Sulyok, M., Krska, R., 2014. Part A-Chem. 31, 2040–2046.
Wu, X., Gao, S., Wang, J.S., Wang, H., Huang, Y.W., Zhao, Y., 2012. Analyst 137 (18), 4226–4234.
Zhao, Y., Yang, Y., Luo, Y., Yang, X., Li, M., Song, Q., 2015. ACS Appl. Mater. Interfaces 7, 21780–21786.